AN EXPERIMENTAL STUDY OF FLAME SPREAD OVER THE BAMBOO SLAB OF DIFFERENT INCLINATION ANGLES AND THICKNESSES

Penghui SUN[1], Kuibin ZHOU[1*], Zhi LI[2*]

[1]College of Safety Science and Engineering, Nanjing Tech University, Nanjing, Jiangsu, 211816, China

[2]College of Civil Engineering and Architecture, Zhejiang University, Hangzhou, Zhejiang, 310058, China

[*] Corresponding author; E-mail: kbzhou@njtech.edu.cn; 17098335700@163.com

Bamboo as a new type of building material, is an alternative raw material for wood and wood-based composites, but its burning could result in fire disaster. The aim of this study was to examine the surface flame spread behavior over the inclined bamboo slab. A series of experiments were conducted using bamboo slabs with thicknesses of 2.5 mm, 3.5 mm, and 5 mm. The flame morphology, flame spread rate, and mass loss rate versus the inclination angle and thickness were measured and physically explained. The results show that the flame spread rate increases with increasing inclination angle of slab and decreases with increasing slab thickness. The mass loss rate is positively affected by the inclination angle, while it is little influenced by the slab thickness. The available flame spread models of thermally thin and thick solid materials underestimate the measured flame spread rates over bamboo slabs. But the thermally thick solid flame spread model is comparatively suitable for the bamboo conditions in this paper. The findings of this study can support the fire permanence design of bamboo structural buildings.

Key words: *flame spread, bamboo, flame morphology, flame spread rate, mass loss rate, inclination angle*

1. Introduction

Bamboo is considered as a new type of building material with great development potential and application prospects [1, 2], due to its short growth cycle, strength, good toughness, and environmental friendliness. The current research on bamboo mainly focuses on the mechanical property [1-4], and clarifies that bamboo has the tensile, flexural, and compressive strength better than softwood and the same strength with hardwood [3]. The bamboo holds the similar chemical composition to the wood that mainly consists of cellulose, hemicellulose, and lignin [4]. Accordingly, bamboo is a combustible material, and its combustion could lead to fire disaster. However, there is relatively little research on the combustion performance and surface flame spread behavior of bamboo, as compared to the wood. The surface flame spread is a common combustion phenomenon in various solid fires, and it is also a key indicator for assessing the combustion performance and fire hazard of building materials. Therefore, it is of great necessity to study the surface flame spread characteristics of bamboo.

The surface flame spread of non-charring solid combustibles has received an intensive study. Ayani and Carmignani [5-7] studied the effect of sample thickness on the downward flame spread of polymethyl methacrylate (PMMA) and found that the flame spread rate decreases to reach a constant with increasing thickness. The pyrolysis length almost linearly increases with the thickness of PMMA [6-8], while the flame spread rate is inversely proportional to the thickness [5, 6, 8], and the mass loss rate per unit width is independent of sample thickness [7]. Zhao *et al*. [9] experimentally found that the flame spread rate over inclined PMMA and polyethylene slabs significantly increases with the increase of inclination angle, due to the increase of pyrolysis length and flame length, as well as the enhancement of heat feedback from the flame to the solid fuel. The flame spread rates are maximum in near-vertical orientations, while mass loss rates are greatest in near-horizontal orientations, for polymetric fuels like PMMA [10]. However, the knowledge or model of flame spread over non-charring materials, could not be applicable to the bamboo.

The current studies of flame spread over charring materials are mainly limited to wood slabs. Chen *et al*. [11] experimentally found that the downward flame spread rate decreases with increasing the thickness of wood slab. The presence of char formation during flame spread can more effectively block the heat conducted toward the interior in the thick wood slabs than in the thin ones, and the char residue ratio affects the accuracy of the flame spread rate model [12]. Zhang *et al*. [13, 14] studied the flame acceleration mechanism and the critical acceleration angle of upward flame spreads, and the flame deceleration mechanism and the critical extinction angle of downward flame spreads over wood slabs. The flame spread is dominated by convective and radiative heat feedback at larger inclination angles, while it is controlled by chemical reactions related to oxygen concentration at smaller angles [15]. The available literature related to the wood surface flame spread can be a good reference for the bamboo flame spread, for bamboo and wood hold similar chemical compositions [1, 2]. However, they have significant differences in microstructure, and the thermal conductivity of bamboo is lower than that of wood [16]. The difference would inevitably affect pyrolysis and heat transfer characteristics, which finally leads to the different flame spread behaviors between bamboo and wood. That is to say, different materials may lead to different characteristic parameters, and it is necessary to obtain burning parameters of bamboo through experiments.

In short, engineering bamboo is widely used for building in China and southeast Asia, and the research on its combustion performance is of great significance for fire prevention. Accordingly, this study experimentally and theoretically investigates the influence of inclination angle and thicknesses on the flame spread over the bamboo slab. The flame morphology, flame spread rate, and mass loss rate were measured and physically explained against the inclination angle and sample thickness. In particular, the comparison of flame spread rate was conducted between model calculation and experimental measurement.

2. Experimental

2.1. Experimental setup and material

The experiment was carried out in a closed space without wind. An experimental setup was designed and constructed to study the flame spread at different inclination angles, as depicted in Fig. 1. The apparatus consisted of a rotatable holder for the bamboo slab, an electronic balance, and a fire-proof plasterboard. The rotatable holder comprised two perforated dials, two splints, and a stainlesssteel frame, as illustrated in Fig. 2. The dials were employed to adjust the slab inclination angle from 0 degree to 180 degree in a 5-degree increment. The upper and lower splints utilized for fixing the slab, help to achieve the upward and downward flame spreads, respectively. The inclination angle was defined as θ and -θ for the upward and downward flame spreads, respectively. In particular, θ=0 indicates the horizontal flame spread.

The rotatable holder was positioned above the electronic balance. Between them was a fire-proof plasterboard that protects the electronic balance from the burning flame. Before ignition, a level gauge was used to calibrate the horizontal placement of the rotatable holder. The electronic balance, with a precision of 0.01 g, was used to record the mass of the bamboo slab. The data acquisition software named CurrentVelocity helps to instantaneously record the slab mass with the sampling frequency of 1 Hz. Two Sony digital cameras (FDR-AXP 55 and FDR-AX 60) were positioned on the right and top, respectively, to capture the flame morphology. The camera had a resolution of 3840 × 2160 pixels with a sampling frequency of 25 Hz. An infrared thermal imager (FOTRI-265), with a precision of 2 ℃, was positioned on the left side of the apparatus to record the ignition temperature of the bamboo surface.

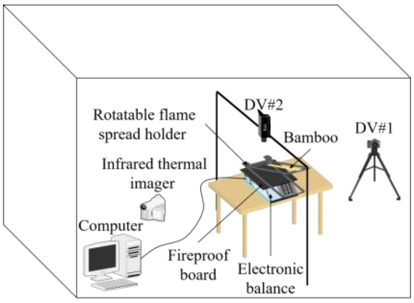

Figure 1. Schematic of the experimental setup

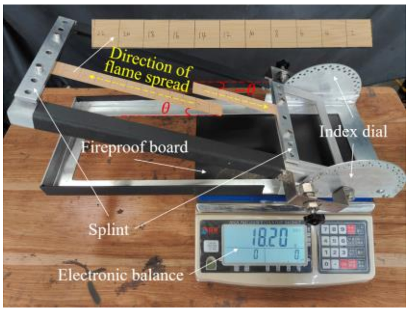

Figure 2. Rotatable holder for the bamboo slab

The bamboo slabs were taken from the engineered bamboo panel as the burning sample, and the scale mark was done for the bamboo slab before ignition (see Fig. 2). The moisture content could affect the test repeatability. Accordingly, the bamboo slab was kept in the oven at a constant 80 ℃ to remove the moisture. The drying process did not stop, until the sample mass reached steady, as shown in Fig. 3. In Fig. 3, M_0 is the initial mass of the bamboo slab, and M is the transient mass of the slab during drying. After the drying, the bamboo slab was placed inside a sealed bag to prevent damping. After the oven dry, the bamboo slab density was 631±41 kg/m^3, and the specific heat capacity and thermal conductivity were 0.8-1.6 kJ/(kg·K) and approximately 0.2 W/(m·K) under ambient temperature, respectively. Tab. 1 listed the test conditions for the bamboo slab. All tests were repeated three times.

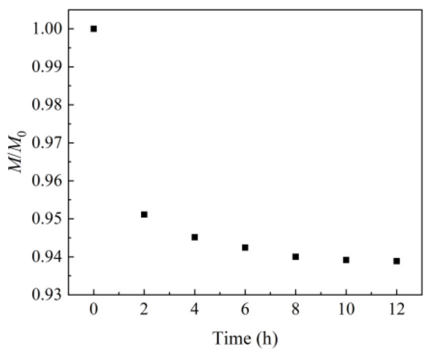

Figure 3. Variation of sample mass with drying time

Table 1. Experimental conditions

Material	Length (mm)	Width (mm)	Thickness (mm)	Inclination angle (°)
Bamboo	120-280	21	2.5, 3.5, 5.0	-20, -15, -10, -5, 0, 10, 20, 30, 60, 90

During the test, the first step is to adjust the inclination angle of the holder, and then the bamboo slab is fixed by the holder and ignited by a linear igniter, and finally the data recording began after the ignition. The linear igniter held the heat power of 301.5 W, with the working voltage and current of 15 V and 20.1 A, respectively. All tests were carried out in still air with the ambient temperature of 25 ℃ ± 2 ℃ and humidity of 40% ± 2%. In particular, the flame spread could not be sustained due to the insufficient heat feedback from the flame to the sample, which is judged by the burning length of less than 6 cm after the removal of the igniter.

2.2. Definition of flame parameters

Figure 4 depicts the characteristic parameters of flame morphology, as the flame spreads over the bamboo slab. The burning sample is divided into the burnout zone (x_b), the pyrolysis zone (x_p), and the preheating zone (δ_p) [13]. The pyrolysis zone is defined as the region where the flame adheres to the sample surface. The preheating zone is defined as the difference between the pyrolysis front and the flame front, i.e., $\delta_p = x_f - x_p$. The flame tilt angle (α) is defined as the angle between the unburned sample surface and the flame centerline.

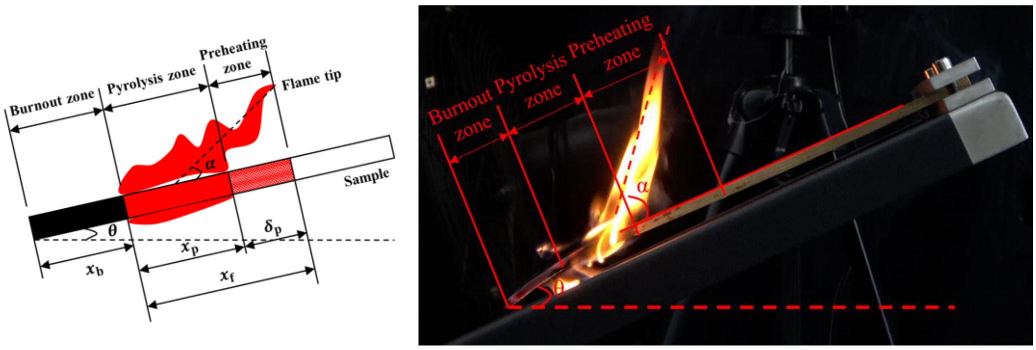

Figure 4. Schematic of flame morphology over the inclined surface

The moving speed of the pyrolysis front position along the sample surface is defined as the flame spread rate (V_f). Figure 5 shows the combustion pattern of the same sample at different times and the unit scales on the sample. Note the lowest point of the U-shape unburned sample used as the division of each combustion region. The flame spread rate can be expressed by:

$$V_f = \frac{x_p(t+\Delta t) - x_p(t)}{\Delta t} \tag{1}$$

where $x_p(t)$ and $x_p(t+\Delta t)$ are the positions of the pyrolysis front at the times of t and ($t+\Delta t$), respectively.

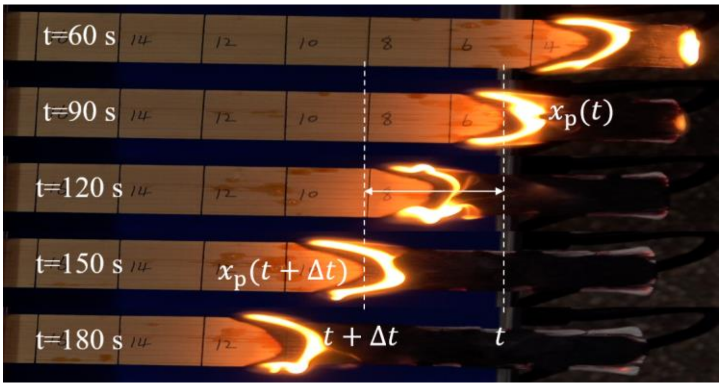

Figure 5. Measurement of flame spread rate. The unit of the scale is centimeter

3. Results and discussions

3.1. Flame morphology

The diffusive combustion reaction between the pyrolysis products and air dominates the flame morphology, which depends on the heat release rate, flame spread rate, and radiation characteristics [17]. Figure 6 shows the flame morphology of the bamboo slabs of 3.5 mm and 5 mm in thicknesses at various inclination angles. As the inclination angle increases, the flame length seems to increase, while the flame tilt angle continuously decreases. In particular, the flame essentially adheres to the sample surface when the inclination angle is 90°.

In the test, the flame appeared on both the upper and lower surfaces of the bamboo slab. The upper surface holds the dominative flame volume when the inclination angle is small. But the lower surface would have an increasing proportion of flame volume, as the inclination angle increases. In particular, the flame is symmetrical on both sides when the inclination angle is 90°. Additionally, the flame encompasses both the pyrolysis and preheating zones of the sample, when the bamboo is 3.5 mm in thickness (Fig. 6(a)). However, the flame only encircles the pyrolysis zone, and is present on both sides of the preheating zone, for the sample of 5 mm in thickness (Fig. 6(b)). Accordingly, in addition to the inclination angle, the sample thickness also considerably affects the flame morphology.

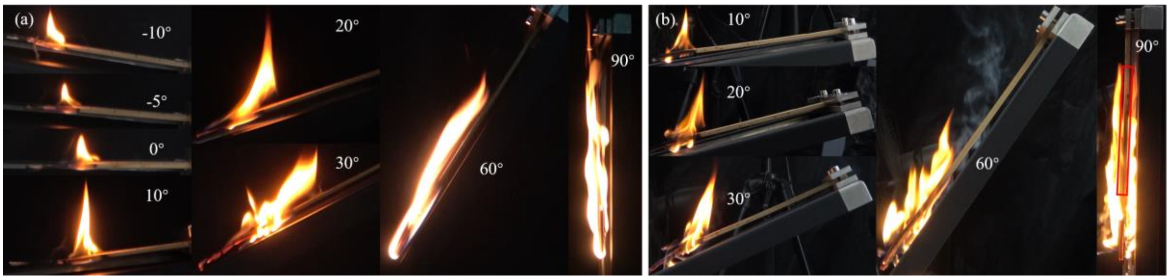

Figure 6. Flame morphology under different inclination angles (a) 3.5 mm, (b) 5.0 mm

In essence, the flame spread on a solid surface is a coupled process of heat and mass transfer between the burning flame and the solid sample. The sample pyrolysis generates the combustible gas to support the flame burning, and the heat necessary for pyrolysis comes from the flame. Figure 7 depicts a schematic diagram to illustrate the heat transfer mechanisms. For the downward flame spread (Fig. 7(a)), the flame tilts towards the burnout zone, due to the pyrolytic gas flow derived by buoyancy force and the stronger air entrainment on the downstream side than the upstream side [18]. The cold air from the downstream side would convectively cool the preheating zone. Additionally, the view factor is little from the flame to the preheating zone. The positive heat feedback depends on the thermal conduction from the pyrolysis zone to the preheating zone. Accordingly, the preheating zone gets a little heat from the flame. For the horizontal flame spread (Fig. 7(b)), the air entrainment shows a balance on both sides of the flame, which reduces the convective cooling effect and increases the view factor to enhance the radiative heat feedback. Consequently, the heat reaching the preheating zone would increase, as compared to that of the downward flame spread. For the upward flame spread (Fig. 7(c)), the flame inclines towards the unburned surface resulting from the Coanda effect [13]. The flame inclination further increases the view factor and causes the convective heating effect to replace the cooling effect on the preheating zone, which significantly enhances the heat feedback. In short, the transition of convective cooling and heating effects, and the enhancement effect of radiative heat feedback, dominate the physical mechanisms for the increase of flame spread rate with the inclination angle.

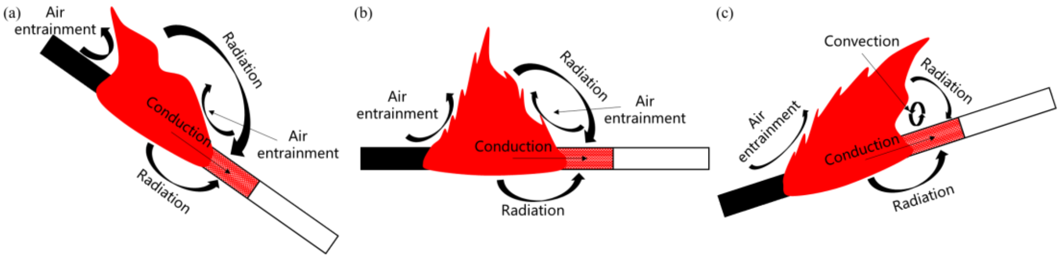

Figure 7. Heat transfer mechanism of flame spread: (a) downward flame spread, (b) horizontal flame spread, (c) upward flame spread

Figure 8 shows the variation of the flame length, pyrolysis length, and flame tilt angle with time for the 3.5 mm thick sample at different inclination angles. The flame length and pyrolysis length show a little decrease as the inclination angle increases from -10° to 0°, but they significantly increase when the inclination angle increases from 0° to 90°. In comparison, the flame tilt angle increases as the inclination angle increases.

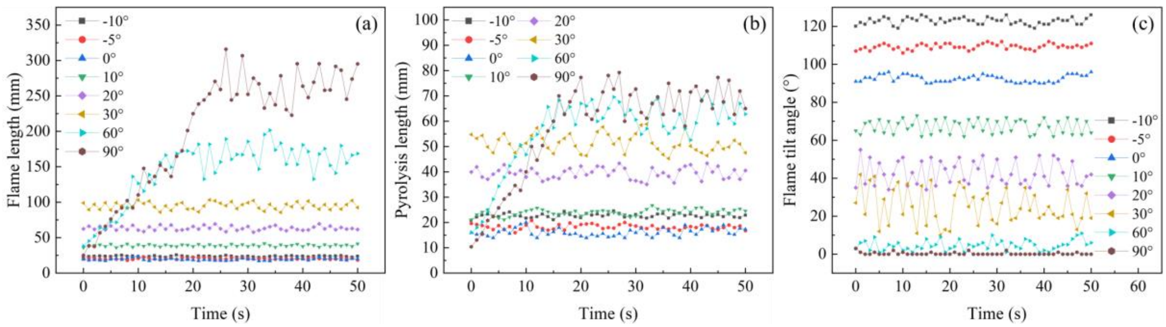

Figure 8. Variation of flame morphology parameters with time: (a) flame length, (b) pyrolysis length, (c) flame tilt angle

The time-averaged flame length, pyrolysis length, flame tilt angle and preheating length are listed in Tab. 2, for the 3.5 mm thick samples of different inclination angles. The time-averaged parameters are only for the flame spread in a quasi-steady period, i.e. 30 s after ignition as shown in Fig. 8. For the upward flame spread, the pyrolysis length and the preheating length increase with the increase of the sample inclination angle. However, the increasing rate of the preheating length is much larger than that of the pyrolysis length.

Table 2. Variation of flame parameters with the sample inclination angle

Sample inclination angle θ (°)	Flame characteristic parameters			
	Flame length x_f (mm)	Pyrolysis length x_p (mm)	Flame tilt angle α (°)	Preheating length δ_p (mm)
-10	23.61	22.68	122.76	0.93
-5	20.24	18.26	109.35	1.98
0	19.15	16.10	92.51	3.05
10	38.89	24.05	67.39	14.84
20	63.33	39.46	42.75	23.87
30	94.94	51.39	25.12	43.55
60	163.42	62.28	4.73	101.14
90	264.72	68.50	0.31	196.22

3.2. Flame spread rate

The flame spread would experience an acceleration before reaching a steady state. Figure 9 depicts the time profile of the pyrolysis front position in the steady state, for the 2.5 mm, 3.5 mm and 5.0 mm thick samples at various inclination angles. The growth rate of the pyrolysis front position over time, i.e., the flame spread rate significantly increases, as the inclination angle increases. It is noteworthy that the flame spread fails, for the 2.5 mm, 3.5 mm and 5.0 mm thick samples of -20°, -15° and 0° inclination angles, respectively. It is of interest to stress that the 3 mm thick wood slab cannot sustain the flame spread for the inclination angle below -20° [15]. The flame can continue to spread over for the 2.5 mm, 3.5 mm and 5.0 mm thick samples of -15°, -10° and 10° inclination angles, respectively. In particular, the flame only spreads 14 cm over the 5.0 mm thick sample of 10° inclination angle. The failure of flame spread results from the weak heat feedback from the burning flame to the preheating zone, especially for the downward flame spread, as discussed in Section 3.1. Additionally, a charring layer would form on the surface of the bamboo slab during the burning, and its thickness increases with the increase of sample thickness. The charring layer can hinder the heat entrance into deeper undecomposed layers of sample and the free release of volatile products into the atmosphere [19]. Accordingly, the hindering effect significantly increases to require a large inclination angle to support the flame spread, as the sample thickness increases.

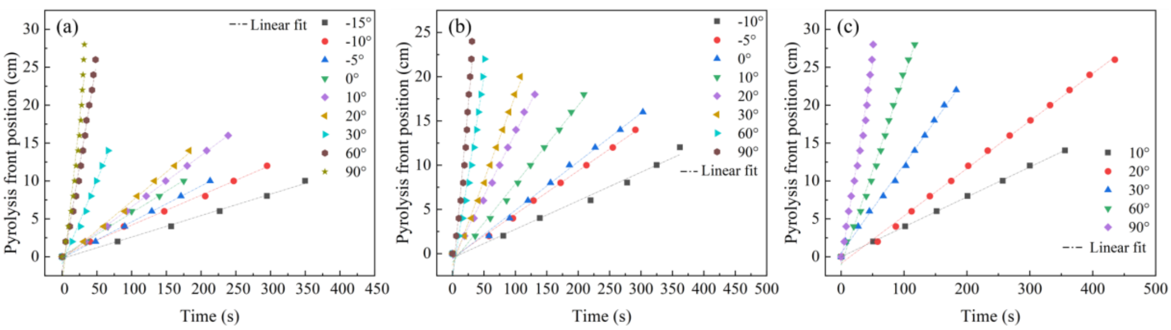

Figure 9. Variation of the position of pyrolysis front with time during the steady flame spread: (a) 2.5 mm, (b) 3.5 mm, (c) 5.0 mm

The position of the pyrolysis front seems to linearly correlate with the time, and thus the variation slope is the flame spread rate. Figure 10 shows the variation of the flame spread rate with the inclination angle for the three thick samples. The flame spread rate increases as the inclination angle increases for all samples. In detail, the downward and upward flame spread rates show a small and significant increase with the inclination angle, respectively. The critical inclination angle is found to be approximately 10° for the transition of flame spread regime from stability to acceleration, which is similar to the surface flame spread of wood paulownia [15].

As discussed in Section 3.1, the conductive heat feedback dominates the flame spread despite the inclination angle, and the radiative heat feedback could slowly increase and the convective cooling effect little reduces as the inclination angle increases, for the downward flame spread. That is why the increase of inclination angle little increases the downward flame spread rate. In comparison, the radiant and convective heating effects significantly increase to accelerate the upward flame spread rate, as the inclination angle increases. Additionally, the decrease of the upward flame spread rate with the sample thickness results from the formation of the surface charring layer. As the sample thickness increases, the thickness of surface charring layer increases to hinder the heat transfer from the surface to the interior, as well as the pyrolysis gas flow from the interior to the surface.

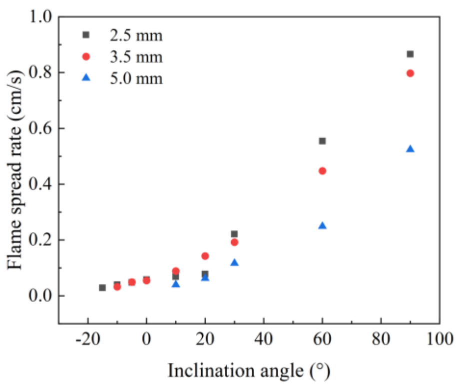

Figure 10. Variation of flame spread rate with inclination angle under different sample thicknesses

3.3. Theoretical calculation of the flame spread rate

De Ris [20] first proposed the opposed-flow flame spread model for the solid material. Later, Quintiere [21] suggested the flame spread models for the thermally thin and thick solid materials, respectively. The key difference between them is the temperature gradient in the thickness direction [12]. The thermally thin solid material can neglect the temperature gradient, while the thermally thick one must consider it.

The basic assumptions for the thermally thin solid material are:

(1) Negligible surface heat loss.

(2) The solid material remains the constant surface temperature (T_∞) when not influenced by the heat flux from the flame.

(3) Steady flame spread (as shown in Fig. 9).

(4) The average heat flux received by the preheating zone is constant.

(5) The heat conduction from the pyrolysis zone to the unburned zone is negligible, i.e., $\dot{q}''_{k,p} = 0$.

The flame spread model for the thermally thin solid material is depicted in Fig. 11(a). The energy conservation equation is given by [21]:

$$\rho c_p d V_f (T_{ig} - T_\infty) = \dot{q}''_f \delta_p \tag{2}$$

where ρ , c_{p}, d, and T_{ig} are the density, specific heat capacity, thickness and ignition temperature of the solid material, respectively; V_{f} is the flame spread rate; T_∞ is the ambient temperature, taken as 298 K; $\dot{q}_{\mathrm{f}}''$ is the average heat flux received by the preheating zone; δ_{p} is the preheating length.

The Eq. (2) gives the flame spread rate expressed by:

$$V_{\mathrm{f}} = \frac{\dot{q}_{\mathrm{f}}''\delta_{\mathrm{p}}}{\rho c_{\mathrm{p}} d(T_{\mathrm{ig}} - T_\infty)} \tag{3}$$

In the thermally thick solid materials, there is a considerable gradient of temperature in the thickness direction. As a result, the control volume cannot select the entire thickness of the solid material for analysis, but it should analyze the thickness region penetrated by the heat. The flame spread model of a thermally thick solid is shown in Fig. 11(b). Its physical model considers a temperature gradient in the y-direction, in addition to the above five assumptions. In particular, $\dot{q}_{\mathrm{f}}'' = 0$ and $T = T_\infty$ at the position of the thermal penetration depth, i.e., $y = \delta_{\mathrm{T}}$.

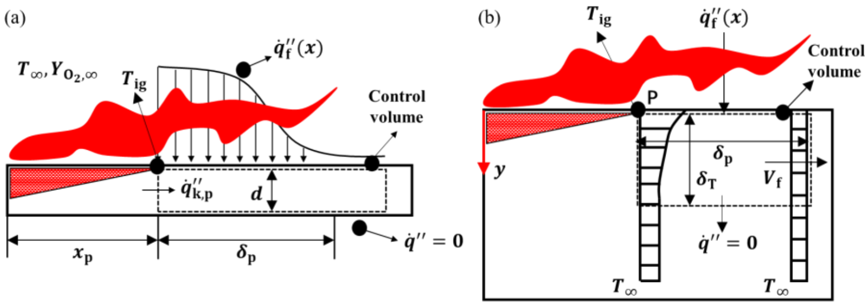

Figure 11. Surface flame spread model of solid material: (a) thermally thin model, (b) thermally thick model

The control volume depicted in Fig. 11(b) pertains to a thermally thick solid in a concurrent-flow mode. Similarly, the findings are also applicable to the opposed-flow mode. The energy conservation equation for the flame spread over the thermally thick solid is given by [21]:

$$\rho c_{\mathrm{p}} V_{\mathrm{f}} \frac{T_{\mathrm{ig}} - T_\infty}{3} C\sqrt{\left(\frac{k}{\rho c_{\mathrm{p}}}\right)\left(\frac{\delta_{\mathrm{p}}}{V_{\mathrm{f}}}\right)} = \dot{q}_{\mathrm{f}}''\delta_{\mathrm{p}} \tag{4}$$

where k is the thermal conductivity of the solid material; C is a dimensionless coefficient of 1 to 4 that depends on T and T_∞. C=2.7 is suggested in the work of Quintiere [22]. Accordingly, the flame spread rate of the thermally thick solid is given by:

$$V_{\mathrm{f}} = \frac{\dot{q}_{\mathrm{f}}''^2 \delta_{\mathrm{p}}}{0.81 k \rho c_{\mathrm{p}} \left(T_{\mathrm{ig}} - T_\infty\right)^2} \tag{5}$$

Notice the validation of assumption (4) only for the horizontal flame spread [21]. Given the variations in the inclination angle of the bamboo slab in this study, the available flame spread model further postulates that the average heat flux received by the preheating zone remains constant despite the inclination angle. Quintiere [22] developed an empirical formula for the heat flux:

$$\dot{q}_{\mathrm{f}}'' = C_{\mathrm{q,L}} BL(\cos\theta L)^{2/5} x_{\mathrm{p}}^{1/5} \tag{6}$$

where $C_{q,L}$, B and L are constant. The Eq. (6) reduces to be $\dot{q}''_f \propto (\cos\theta)^{2/5} x_p^{1/5}$. Note that the inclination angle of 90° cannot be considered, for cos90°=0. The correlation between the $(\cos\theta)^{2/5} x_p^{1/5}$ and the inclination angle is depicted in Fig. 12. As shown, $(\cos\theta)^{2/5} x_p^{1/5}$ ranges from 0.43 to 0.52, in the inclination angle range of -10° to 60°. Accordingly, the average heat flux received by the preheating zone can be approximated as a constant. That is to say, assumption (4) is still reasonable despite the inclination angle of sample.

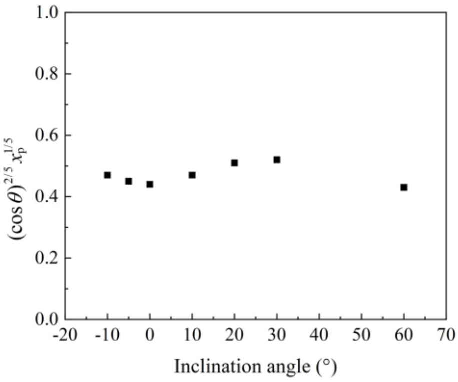

Figure 12. $(\cos\theta)^{2/5} x_p^{1/5}$ as a function of inclination angle

Morrisset *et al.* [23] proposed the average heat fluxes of 18.5 kW/m^2, 17.8 kW/m^2, and 19.5 kW/m^2 for the downward, horizontal, and lateral spread of PMMA, respectively. Saito *et al.* [24] reported an average heat flux of 25 kW/m^2 for the upward spread of Douglas-fir. Given that bamboo is a charring material similar to Douglas-fir, 25 kW/m^2 is adopted to approximate the average heat flux in the preheating zone in this study. The thermophysical parameters of bamboo are listed in Tab. 3. The density, specific heat capacity and thermal conductivity are measured for model calculation. Notice the specific heat capacity of 1.48 kJ/(kg·K) [25] and the thermal conductivity of 0.19 W/(m·K) [26] for moso bamboo. The ignition temperature of 380 ℃ used for model calculation, is the mean value of laminated bamboo samples measured by the Cone Calorimeter [27].

Table 3. Thermophysical parameters of bamboo

Density ρ (kg·m^{-3})	Specific heat capacity c_p (kJ·kg^{-1}·K^{-1})	Thermal conductivity k (W·m^{-1}·K^{-1})	Ignition temperature [27] T_{ig} (℃)
631±41	1.2±0.4	0.2	380±8

The Eqs. (3) and (5) can used to calculate the flame spread rates for the thermally thin and thick solid materials, respectively. Figure 13 shows the comparison of the flame spread rate between the model calculation and the experimental measurement. Equation (3) underestimates all the flame spread rates under different inclination angles, while Eq. (5) underestimates most of the flame spread rates. In particular, the underestimation of Eq. (3) is more significant than that of Eq. (5). The prediction errors of Eq. (3) largely exceed 20%, while those of Eq. (5) are less than 20%. In short, the thermally thick solid material seems relatively reasonable to approximate the bamboo slab in this study. The Eq. (5) gives a better prediction on the flame spread rate for the 5 mm thick bamboo slab, as compared to those of the 2.5 mm and 3.5 mm thick ones, as indicated in Fig. 13(b). As observed in Fig. 6(b), the thermal penetration depth would be much less than the sample thickness, as the sample is thick enough. Accordingly, as the bamboo slab thickness increases, the prediction of Eq. (5) gradually approaches the measurement.

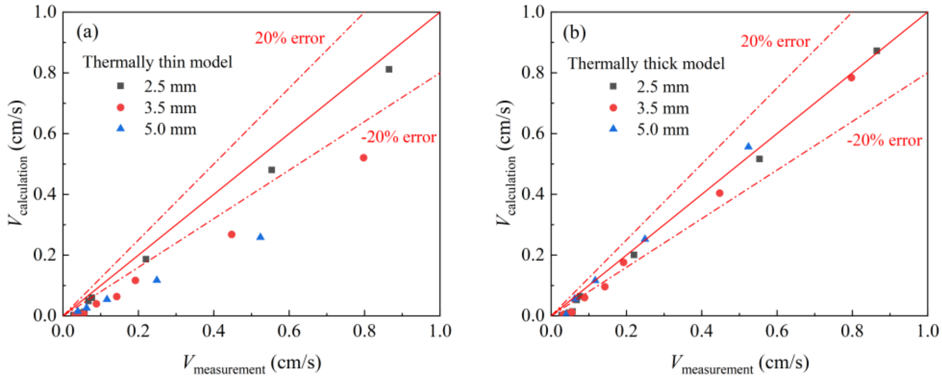

Figure 13. Comparison of flame spread rate between the measurement and the calculation of (a) thermally thin model and (b) thermally thick model

In both models, the omission of heat conduction from the pyrolysis zone to the preheating zone results in the underestimation of the flame spread rate. Moreover, both models solely consider the heat flux from the flame over the upper surface to the preheating zone. As evidenced in Fig. 6, the flame is also present on the lower surface of the bamboo slab, and it also imposes a positive influence on the flame spread rate, especially for large inclination angles.

Figure 14(a) displays the surface temperature of bamboo slab measured by the infrared thermal imager. Figure 14(b) depicts the variation of the maximum temperature on the sample surface with time at different inclination angles. The maximum surface temperature fluctuates around 600 ℃ during the flame spread, which significantly exceeds the ignition temperature of bamboo slab, i.e. approximately 380 ℃ [27]. Accordingly, the actual heat flux received by the preheating zone exceeds the assumed heat flux in the flame spread model. This discrepancy also contributes to the underestimation of the flame spread rate by theoretical models.

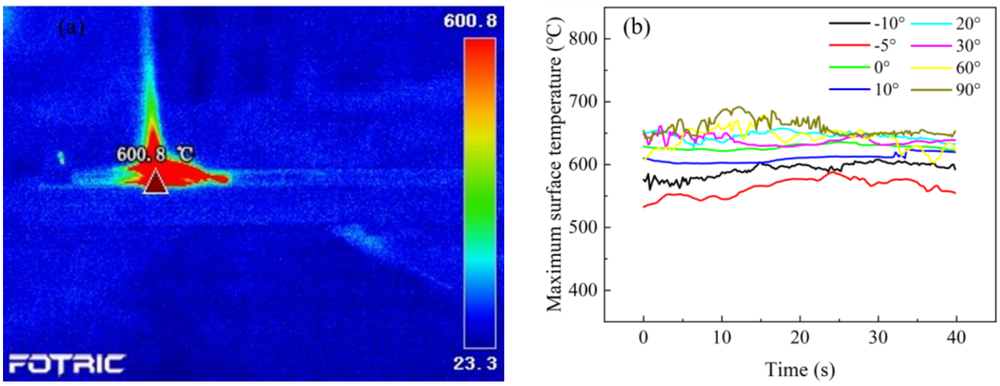

Figure 14. Surface ignition temperature of bamboo slab: (a) infrared thermogram, (b) maximum surface temperature as a function of time

3.4. Mass loss rate

The mass loss rate which indicates the reduction in mass per unit time during flame spread, is a crucial factor to characterize the combustion intensity. Figure 15 shows the variation of sample mass with time during the flame spread at different inclination angles. The sample mass is normalized by the initial sample mass (M_0). The variation of sample mass is nonlinear during the initial period, and then reaches linear after the flame spread achieves steady. In addition, the variation slope of sample mass with time increases, as the inclination angle increases.

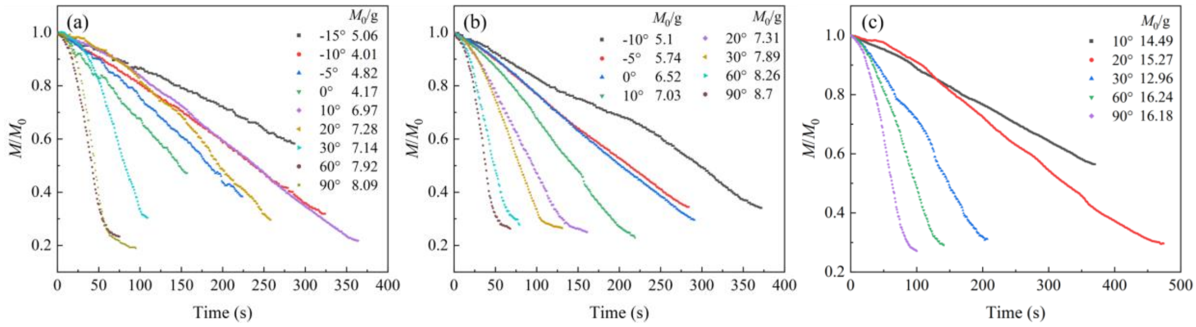

Figure 15. Variation of normalized sample mass with time under different inclination angles: (a) 2.5 mm, (b) 3.5 mm, (c) 5.0 mm

The variation slope of sample mass with time defines the mass loss rate in the steady flame spread. Figure 16 shows the variation of the mass loss rate with the inclination angle for the three thick samples. The comparison between Figs. 10 and 16 shows that the mass loss rate and the flame spread rate hold the same variation trend with the inclination angle. However, the effect of the sample thickness is little on the mass loss rate, as compared to that on the flame spread rate. Experimental results of downward flame spread over PMMA also show that the mass loss rate per unit width is independent of sample thickness [7]. There is no doubt that more heat is available for the pyrolysis as the inclination angle increases, which increases the mass loss rate of the bamboo slab. The mass loss rate can be rudely estimated by the product of the flame spread rate, cross-sectional area, and density of the bamboo slab. The density and width are constant for the three thick samples in this study, and the flame spread rate is inversely proportional to the sample thickness, as indicated in Fig. 10. Accordingly, the mass loss rate that depends on the product of the flame spread rate and sample thickness, could be little affected by the sample thickness.

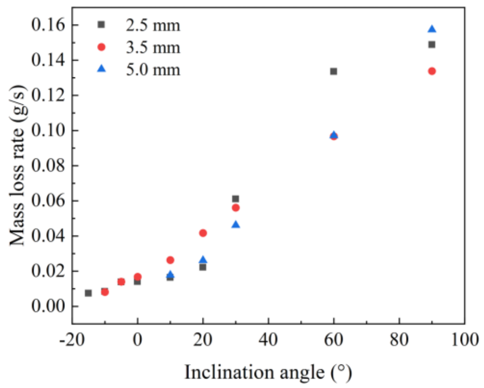

Figure 16. Variation of mass loss rate with inclination angle

4. Conclusions

This paper systematically studies the flame spread behavior over the bamboo slab by experimental simulation and theoretical analysis. The physical explanation is conducted for the effect of slab inclination angle and thickness on the flame morphology, flame spread rate, and mass loss rate. The major findings include:

The inclination angle and thickness significantly affect the flame morphology, by which the transition occurs between convective cooling and heating effects and the radiative heating effect is enhanced by increasing the inclination angle.

The flame spread rate increases with the increase in the inclination angle and decreases with the increase in sample thickness. The mass loss rate also increases with the inclination angle, but the effect of sample thickness on the mass loss rate is relatively minor.

The available flame spread models of thermally thin and thick solid materials underestimate the flame spread rate over the bamboo slab. However, the thermally thick solid flame spread model is comparatively suitable for the conditions in this study. The flame spread models neglect the heat conduction from the pyrolysis zone to the preheating zone and the influence of the lower surface flame on the flame spread over the bamboo slab. However, combustion experiments of scale-different bamboo slabs should be carried out to clear the boundary of the available models in the future.

Acknowledgement

This work was supported by the National Natural Science Foundation of China under Grant nos. 51506082 and 51876088. K.Z. acknowledges the support from the Six Talent Peaks Project of Jiangsu Province of China under Grant no. XNYQC-005.

References

[1] Qiu, Z. Y., Fan, H. L., Laminated bamboo materials for plated building structures, *Journal of Building Engineering*, *61* (2022), 105239

[2] Hong, C. K., *et al*., Review of connections for engineered bamboo structures, *Journal of Building Engineering, 30* (2020), 101324

[3] Verma, C. S., *et al*., Comparative study of mechanical properties of bamboo laminae and their laminates with woods and wood based composites, *Composites Part B: Engineering*, *60* (2014), pp. 523-530

[4] Kelkar, B. U., *et al*., Structural bamboo composites: A review of processing, factors affecting properties and recent advances, *Advances in Bamboo Science, 3* (2023), 100026

[5] Ayani, M. B., *et al*., Downward flame spread over PMMA sheets in quiescent air: experimental and theoretical studies, *Fire Safety Journal, 41* (2006), pp. 164-169

[6] Carmignani, L., *et al*., Correlation of burning rate with spread rate for downward flame spread over PMMA, *Fire Technology, 54* (2018), pp. 613-624

[7] Carmignani, L., Bhattacharjee, S., Burn angle and its implications on flame spread rate, mass burning rate, and fuel temperature for downward flame spread over thin PMMA, *Combustion Science and Technology, 192* (2019), pp. 1617-1632

[8] Bhattacharjee, S., *et al*., Correlating the burning rate with spread rate for downward flame spread over PMMA, in: 10^{th} U. S. National Combustion Meeting, 2017

[9] Zhao, K., *et al*., Experimental study on flame spread over inclined PMMA and PE slabs, *Key Engineering Materials, 775* (2018), pp. 390-394

[10] Gollner, M. J., *et al*., Experimental study of upward flame spread of an inclined fuel surface, *Proceedings of the Combustion Institute, 34* (2013), pp. 2531-2538

[11] Chen, P., *et al*., Behavior of flame spread downward over thick wood sheets and heat transfer analysis, *Journal of Fire Sciences, 25* (2016), pp. 5-21

[12] Hong, T.-K., Park, S.-H., Influences of the presence of char layer on flame spreads over wood with different thermal thickness, *Journal of Mechanical Science and Technology, 37* (2023), pp.3841-3848
[13] Zhang, Y., *et al*., Prediction of the critical condition for flame acceleration over wood surface with different sample orientations, *Combustion and Flame, 159* (2012), pp. 2999-3002
[14] Zhang, Y., *et al*., The deceleration mechanism and the critical extinction angle of downward flame spread over inclined cellulosic solids, *Applied Thermal Engineering, 124* (2017), pp. 185-190
[15] Wang, Q. S., *et al*., Flame spread on inclined wood surfaces: influence of external heat flux and ambient oxygen concentration, *Combustion Science and Technology, 190* (2017), pp. 97-113
[16] Shah, D. U., *et al*., Thermal conductivity of engineered bamboo composites, *Journal of Materials Science, 51* (2016), pp. 2991-3002
[17] Rangwala, A. S., *et al*., Upward flame spread on a vertically oriented fuel surface: The effect of finite width, *Proceedings of the Combustion Institute, 31* (2007), pp. 2607-2615
[18] Zhang, G. H., *et al*., Deceleration mechanism of downward flame spreading over inclined solid surface based on FireFOAM, *Case Studies in Thermal Engineering, 34* (2022), 102066
[19] Mačiulaitis, R., *et al*., Research of natural wood combustion and charring processes, *Journal of Civil Engineering and Management, 18* (2012), pp. 631-641
[20] De Ris, J. N., Spread of a laminar diffusion flame, *Proceedings of the Combustion Institute, 12* (1969), pp. 241-245
[21] Quintiere, J. G., *Fundamentals of fire phenomena*, John Wiley & Sons, 2006
[22] Quintiere, J. G., The effects of angular orientation on flame spread over thin materials, *Fire Safety. Journal., 36* (2001), pp. 291-312
[23] Morrisset, D., *et al*., Characterization of flame spread over PMMA using a temperature reconstruction method, *Combustion Science and Technology, 195* (2023), pp. 3557-3570
[24] Saito, K., *et al*., Upward turbulent flame spread, *Fire Safety Science, 1* (1986), pp. 75-86
[25] Huang, P. X., *et al*., Specific heat capacity measurement of Phyllostachys edulis (Moso bamboo) by differential scanning calorimetry, *Construction and Building Materials, 125* (2016), pp. 821-831
[26] Huang, P. X., *et al*., Heat and moisture transfer behaviour in Phyllostachys edulis (Moso bamboo) based panels, *Construction and Building Materials, 166* (2018), pp.35-49
[27] Solarte, A., *et al*., Understanding fire growth for performance based design of bamboo structures, *Fire Safety Journal, 120* (2021), 103057

Submitted: 24.02.2024.
Revised: 18.05.2024.
Accepted: 22.05.2024.